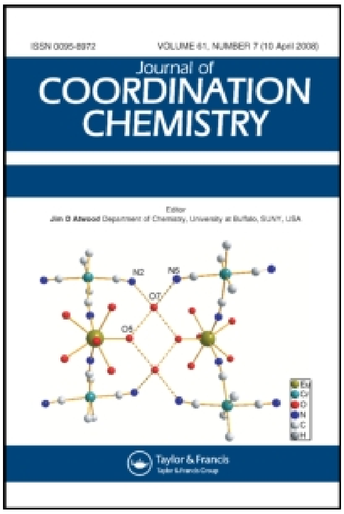

Journal of Coordination Chemistry
Publication details, including instructions for authors and subscription information:
http://www.informaworld.com/smpp/title~content=t713455674

Metal complexes of 2-benzoylpyridine-derived thiosemicarbazones: structural, electrochemical and biological studies

Ricardo F. F. Costa[a]; Anayive P. Rebolledo[a]; Túlio Matencio[a]; Hállen D. R. Calado[a]; José D. Ardisson[b]; Maria E. Cortés[a]; Bernardo L. Rodrigues[c]; Heloisa Beraldo[a]
[a] Departamento de Química, Universidade Federal de Minas Gerais, Belo Horizonte Minas Gerais, Brazil [b] Centro de Desenvolvimento da Tecnologia Nuclear, CDTN, Belo Horizonte, Minas Gerais, Brazil [c] Instituto de Física de São Carlos, Universidade de São Paulo, São Carlos, São Paulo, Brazil

To cite this Article Costa, Ricardo F. F. , Rebolledo, Anayive P. , Matencio, Túlio , Calado, Hállen D. R. , Ardisson, José D. , Cortés, Maria E. , Rodrigues, Bernardo L. and Beraldo, Heloisa(2005) 'Metal complexes of 2-benzoylpyridine-derived thiosemicarbazones: structural, electrochemical and biological studies', Journal of Coordination Chemistry, 58: 15, 1307 — 1319

To link to this Article: DOI: 10.1080/00958970500213307

URL: http://dx.doi.org/10.1080/00958970500213307

Journal of Coordination Chemistry
Vol. 58, No. 15, October 2005, 1307–1319

Taylor & Francis
Taylor & Francis Group

Metal complexes of 2-benzoylpyridine-derived thiosemicarbazones: structural, electrochemical and biological studies

RICARDO F. F. COSTA†, ANAYIVE P. REBOLLEDO†, TÚLIO MATENCIO†,
HÁLLEN D. R. CALADO†, JOSÉ D. ARDISSON‡, MARIA E. CORTÉS§,
BERNARDO L. RODRIGUES¶ and HELOISA BERALDO*†

†Departamento de Química, Universidade Federal de Minas Gerais, 31270-901,
Belo Horizonte Minas Gerais, Brazil
‡Centro de Desenvolvimento da Tecnologia Nuclear, CDTN, 31270-901,
Belo Horizonte, Minas Gerais, Brazil
§Faculdade de Odontologia, Universidade Federal de Minas Gerais, 31270-901,
Belo Horizonte Minas Gerais, Brazil
¶Instituto de Física de São Carlos, Universidade de São Paulo, Caixa Postal 369,
13560-970, São Carlos, São Paulo, Brazil

(*Received 27 August 2004; revised 4 October 2004; in final form 3 April 2005*)

Complexes of 2-benzoylpyridine thiosemicarbazone (H2Bz4DH) as well as of its N(4)-methyl (H2Bz4Me) and N(4)-phenyl (H2Bz4Ph) analogues with iron(II), nickel(II) and zinc(II) were characterized by a variety of spectroscopic techniques. Electrochemical studies revealed that the iron(II) complexes undergo oxidation giving the iron(III) analogues, which could be reduced back by cellular thiols such as thioredoxine, suggesting that this process could occur in biological media. The thiosemicarbazones have antifungal activity against *Candida albicans* that significantly decreases on coordination. The crystal structure 2-benzoylpyridine-N(4)-methyl thiosemicarbazone (H2Bz4Me) was determined.

Keywords: 2-Benzoylpyridine thiosemicarbazones; Metal complexes; Biological activity

1. Introduction

Thiosemicarbazones and their metal complexes have shown pharmacological applications and have been evaluated for antitumoral, antibacterial and antifungal properties among others [1, 2]. Antitumoral action of $\alpha(N)$-heterocyclic thiosemicarbazones (HTCs) occurs by inhibiting DNA syntheses through the blockage of the enzyme

---

*Corresponding author. Fax: 553134995700. Tel.: 553134995740. Email: hberaldo@ufmg.br

Journal of Coordination Chemistry
ISSN 0095-8972 print: ISSN 1029-0389 online © 2005 Taylor & Francis
DOI: 10.1080/00958970500213307

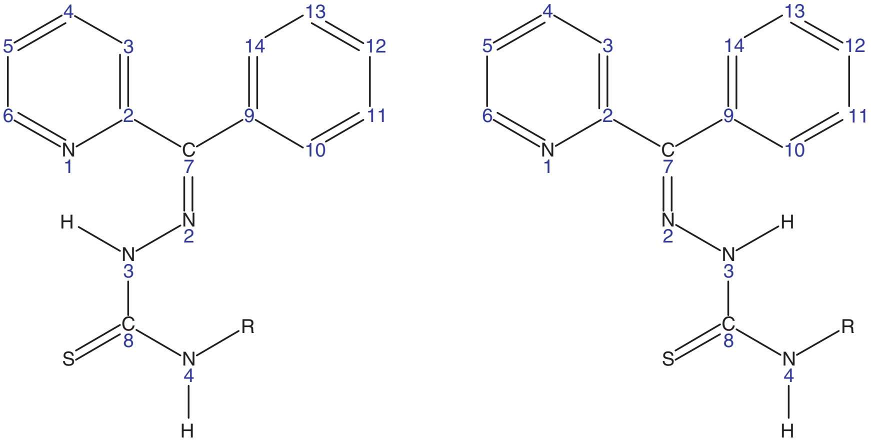

Figure 1. Structures of 2-benzoylpyridine thiosemicarbazones: H2Bz4DH, R = H; H2Bz4Me, R = methyl; H2Bz4Ph, R = phenyl. *Z* (left) and *E* (right) configurational isomers.

ribonucleoside diphosphate reductase (RDR), which catalyses the conversion of ribonucleotides into deoxyribonucleotides. The inhibitory species is an iron-HTC complex [3].

Thiosemicarbazones derived from 2-formyl and 2-acetylpyridine have been extensively investigated [4–9]. Though, much less attention has been given to those derived from 2-benzoylpyridine. For the latter, a series of metal complexes with the unsubstituted derivative has been prepared, and the antibacterial activity of the ligand and its complexes have been investigated [10]. Copper(II) complexes with N(4)-alkyl derivatives [11, 12] have been studied as well as a few nickel(II) and cobalt(II,III) complexes with the N(4)-cyclohexyl derivative [13].

Some N(4)-dialkyl-2-benzoylpyridine thiosemicarbazones and their copper(II) complexes are active against the human pathogenic fungi *Aspergillus niger* and *Paecilomyces variotii* [11]. In a recent publication tin(IV) complexes of N(4)-phenyl-2-benzoylpyridine thiosemicarbazone (H2Bz4Ph), which had antifungal activity against *Candida albicans*, have been studied [14].

In the present work iron(II), nickel(II) and zinc(II) complexes of 2-benzoylpyridine thiosemicarbazone (H2Bz4DH) as well as N(4)-methyl (H2Bz4Me) and N(4)-phenyl (H2Bz4Ph) analogues were studied (figure 1). An electrochemical study of the iron complexes was carried out and the antifungal activity of the thiosemicarbazones and their metal complexes was tested against *Candida albicans*.

2. Experimental

The thiosemicarbazones were prepared as described in the literature [11–13]. Metal complexes were obtained by refluxing an EtOH solution of the ligand with iron(II), nickel(II) or zinc(II) chloride (anhydrous) for 5–6 h in 2 : 1 ligand-to-metal molar ratio. The solids were washed with EtOH then ether, and dried *in vacuo*. The percentage yields (%) were: 70 (**1**); 56 (**2**); 50 (**3**); 68 (**4**); 56 (**5**); 54 (**6**); 57 (**7**); 51 (**8**); 49 (**9**) (see table 1).

Table 1. Colours, partial elemental analyses and molar conductivities of the Fe(II), Ni(II) and Zn(II) complexes of 2-benzoylpyridine thiosemicarbazones.

		Found (Calcd) (%)			
Compound	Colour	C	H	N	Λ_M[a]
[Fe(H2Bz4DH)$_2$]Cl$_2$ (**1**)	Violet	47.94 (48.85)	3.75 (3.78)	17.05 (17.52)	138.6
[Fe(H2Bz4Me)$_2$]Cl$_2$ (**2**)	Violet	49.35 (50.40)	4.13 (4.19)	17.15 (16.78)	141.7
[Fe(H2Bz4Ph)$_2$]Cl$_2$ (**3**)	Black	58.37 (57.67)	3.98 (4.08)	13.80 (14.15)	140.2
[Ni(2Bz4DH)Cl] (**4**)	Brown	45.58 (44.69)	3.55 (3.65)	16.03 (16.39)	32.6
[Ni(2Bz4Me)Cl] (**5**)	Brown	45.95 (46.28)	3.60 (3.68)	15.32 (15.41)	38.0
[Ni(H2Bz4Ph)$_2$]Cl$_2$ (**6**)	Brown	58.01 (57.47)	3.94 (4.06)	14.19 (14.10)	128.5
[Zn(H2Bz4DH)$_2$Cl$_2$] (**7**)	Yellow	47.31 (48.07)	3.82 (3.73)	17.75 (17.25)	16.3
[Zn(H2Bz4Me)$_2$Cl$_2$] (**8**)	Yellow	48.44 (49.70)	4.11 (4.14)	16.62 (16.57)	18.1
[Zn(H2Bz4Ph)Cl$_2$] (**9**)	Yellow	48.69 (48.72)	3.45 (3.42)	11.89 (11.97)	20.6

[a] 10^{-3} mol L^{-1} in DMF (Ω^{-1} cm^2 mol^{-1}).

Infrared spectra were recorded on a Perkin-Elmer 283B spectrometer using nujol mulls between CsI plates. NMR spectra were obtained with a Brucker DRX-400 Avance (400 MHz) spectrometer using deuterated dimethyl sulfoxide (DMSO-d$_6$) as the solvent and tetramethylsilane (TMS) as internal reference. Partial elemental analyses were obtained with a Perkin-Elmer PE 2400 analyser. An YSI model 31 conductivity bridge was employed for molar conductivity measurements. Mössbauer spectra were obtained using a conventional constant acceleration spectrometer, moving a ^{57}Co/Rh source at room temperature. Electronic spectra were acquired with a Hewlett Packard 8453 spectrometer in dimethyl formamide (DMF) solutions using 1 cm cells.

Electrochemical experiments were performed at room temperature with Autolab Eco Chemie Pgstat 30 equipment. Measurements were obtained using cyclic voltammetry. The electrochemical cell consisted of a glass container with a cap having holes for a three-electrode configuration and nitrogen. Platinum electrodes were employed as working and auxiliary electrodes and Ag/AgNO$_3$ (0.1 mol L^{-1} in acetronitrile) was used as the reference electrode. The supporting electrolyte in DMF was tetrabutylammonium tetrafluoroborate (0.1 mol L^{-1}) and solutions were 1×10^{-3} mol L^{-1} in all complexes. All measured potentials are relative to the normal hydrogen electrode (NHE) using the reversible ferrocene/ferrocenium couple (+0.400 V *vs.* NHE, $\Delta E_p = 90$ mV at 100 mV s^{-1}) as a standard.

The structure of H2Bz4Me was investigated by single crystal X-ray diffraction. Data were collected at 293 K using a Kappa CCD diffractometer. Monochromated Mo-K_α radiation ($\lambda = 0.71073$ Å) was used. The Collect package [15] was used for data collection. Lattice parameters were obtained by least squares fit from 3054 reflections measured with θ between 1.0 and 27.5°. Intensities were measured for 5836 reflections, 3082 independent; 2447 with $I > 2\sigma(I)$ were used in the structure determination and refinements. The HKL Denzo and Scalepack programs [16] were used for cell refinement and data reduction. The SHELXS and SHELXL programs [17, 18] were used to solve and refine the structure.

Candida albicans (ATCC 18804) liquid cultures were prepared in Sabouraud Dextrose Broth. The cultures were incubated at 37°C for 24 h. The agar disc diffusion method for assaying antifungal activity was used.

Table 2. Crystal data and refinement results for H2Bz4Me.

Crystal data	
Compound	H2Bz4Me
Empircal formula	$C_{14}H_{14}N_4S$
Formula weight	270.36
Crystal system	Monoclinic
Space group	$P2_1/c$
a (Å)	9.2957(4)
b (Å)	13.5886(6)
c (Å)	11.1285(6)
β (°)	103.084(2)
V (Å^3)	1369.21(11)
Z	4
ρ (Mg m^{-3})	1.312
Radiation (Å)	Mo-K$_\alpha$, 0.71073
μ (mm^{-1})	0.228
Color; habit	Yellow; prism
Crystal size (mm^3)	$0.29 \times 0.28 \times 0.25$
Absorption correction	None
Data collection	
Diffractometer	Nonius kappa CCD
T (K)	293(5)
Completeness (%)	98.5
θ range (°)	$1 < \theta < 27.5$
d$_{hkl}$ range (Å)	$1.54 < d_{hkl} < 41.00$
(h k l) range	$-12 \leq h \leq 12$, $-17 \leq k \leq 17$, $-14 \leq l \leq 14$
Collected reflections	5836
Independent reflections	3082
R_{int}	0.024
Refinement	
Observed reflections ($I \geq 2\sigma(I)$)	2447
R_1 (obs/all)	0.0456/0.0613
wR_2 (obs/all)	0.1155/0.1266
Goodness-of-fit	1.082
Larg. diff. peak/hole (e Å^{-3})	0.202, −0.235

3. Results and discussion

3.1. *Crystal structure of H2Bz4Me*

Crystal data and refinement results for H2Bz4Me are listed in table 2. Perspective views for the asymmetric unit of H2Bz4Me can be seen in figures 2(a) and (b).

The *Z* configuration of H2Bz4Me in the crystal is stabilized by an intramolecular hydrogen bond between N3–H3 and the heteroaromatic nitrogen (figure 2a). Among other forces, the crystalline solid is stabilized by an intermolecular hydrogen bond between N4–H4 of one molecule and S1 of a neighbouring molecule, forming an infinite chain of H2Bz4Me molecules, as shown in figure 2(b). The crystal structure of H2Bz4Ph, previously determined also revealed the presence of the *Z* configuration in the solid [14]. However, H4Bz4Ph, in which the side chain is attached to the four-position in the pyridine ring, crystallizes in the *E* configuration, which is preferred if no N3–H3–N1 hydrogen bonding can occur [19].

As expected, bond distances in H2Bz4Me are very similar to those of H2Bz4Ph [14] and also not much different from those determined for H4Bz4Ph [19]. The most

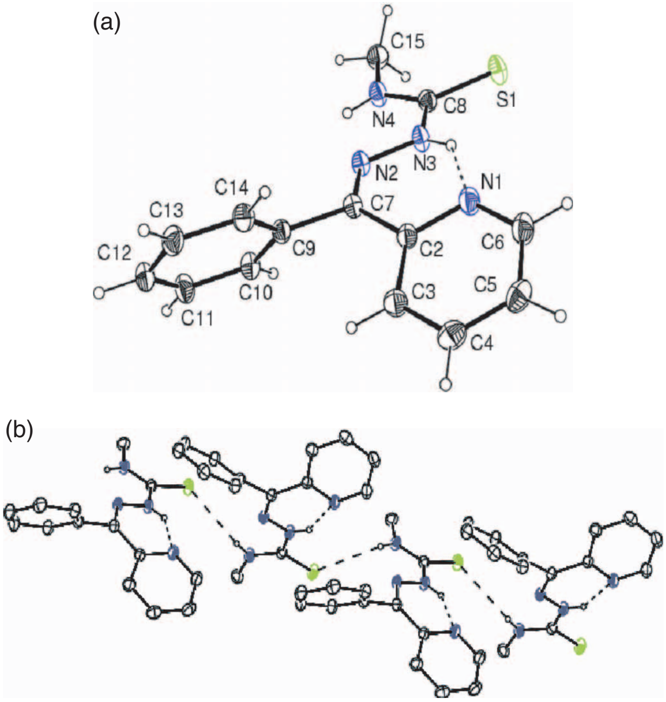

Figure 2. (a) The molecule of H_2Bz_4Me, and (b) the infinite chain of molecules in the crystal linked by N4–H4–S1 intermolecular hydrogen bonds. Aromatic and methyl hydrogens are omitted for clarity.

significant differences are in the S1–C8 distance which is 1.680(2) Å in H2Bz4Me and 1.663(2) Å in H2Bz4Ph, C8–N4, which is 1.323(2) Å in H2Bz4Me and 1.343(3) Å in H2Bz4Ph, and N4–C15, which is 1.449(2) Å in H2Bz4Me and 1.410(2) Å in H2Bz4Ph. Those differences are probably due to the different electronic and steric effects of the methyl and phenyl substituents at N4. In fact, the electron-withdrawing effect of the phenyl group seems to strengthen the C–S double bond whereas the electron-donating effect of the methyl group makes this bond slightly weaker. The consequences of these effects are reversed on the C8–N4 bond, which is weaker in H2Bz4Ph than in H2Bz4Me. The variations in N4–C15 are due to the differences in the nature of C15 (from a methyl or from a phenyl group). The other bond distances are practically if not exactly the same.

Variations in angles within the lateral chain in the two compounds are observed only in the vicinity of N4, as a consequence of the different groups attached to this nitrogen. Hence the C8–N4–C15 angle is 124.1(2)° in H2Bz4Me but 130.4(2)° in H2Bz4Ph, the N4–C8–S angle is 124.7(2)° in H2Bz4Me but 128.0(1)° in H2Bz4Ph and the N4–C8–N3 angle is 116.7(2)° in H2Bz4Me and 114.3(2)° in H2Bz4Ph.

Table 1 lists the colours, partial elemental analyses and molar conductivities of the complexes. The data indicate the formation of $[Fe(HL)_2]Cl_2$ complexes with all three thiosemicarbazones, in which HL stands for the neutral ligand. The syntheses with nickel(II) chloride give either a 2 : 1 ligand-to-metal complex, $[Ni(HL)_2]Cl_2$, with H2Bz4Ph, or 1 : 1 [Ni(L)Cl] complexes (L = anionic ligand) with H2Bz4DH or H2Bz4Me. In the latter, deprotonation upon complexation occurs and a chloride ion

Table 3. Infrared absorptions (cm^{-1}) of 2-benzoylpyridine thiosemicarbazones and their Fe(II), Ni(II) and Zn(II) complexes.

Compound	ν(C=N)	ν(C=S)	ρ_{py}	ν(M–N)	ν(M–S)	ν(M–Cl)	ν(M–N$_{py}$)
H2Bz4DH	1615s	805w	595m	–	–	–	–
H2Bz4Me	1585s	800s	595m	–	–	–	–
H2Bz4Ph	1590s	800m	590m	–	–	–	–
[Fe(H2Bz4DH)$_2$]Cl$_2$ (**1**)	1575s	797w	650w	417m	360w	–	280w
[Fe(H2Bz4Me)$_2$]Cl$_2$ (**2**)	1560w	788w	655w	420w	357w	–	285w
[Fe(H2Bz4Ph)$_2$]Cl$_2$ (**3**)	1565s	780m	653w	406m	358w	–	293w
[Ni(2Bz4DH)Cl] (**4**)	1595s	758m	640m	450m	360m	302w	277w
[Ni(2Bz4Me)Cl] (**5**)	1575s	749m	655m	470m	350m	302m	280m
[Ni(H2Bz4Ph)$_2$]Cl$_2$ (**6**)	1560s	790m	590m	420m	375m	–	–
[Zn(H2Bz4DH)$_2$Cl$_2$] (**7**)	1595s	785m	605s	398w	360w	254w	–
						280m	–
[Zn(H2Bz4Me)$_2$Cl$_2$] (**8**)	1575s	790m	600m	374w	340m	254w	–
						280m	–
[Zn(H2Bz4Ph)Cl$_2$] (**9**)	1560s	790s	588w	345m	335m	254w	–
						280m	–

Note: s, strong; m, medium; w, weak.

acts as a ligand occupying the fourth coordination position, as suggested by the molar conductivity measurements. Reaction of the 2-benzoylpyridine thiosemicarbazones with zinc(II) chloride produces either 2 : 1 ligand-to-metal complexes, [Zn(HL)$_2$Cl$_2$], with H2Bz4DH or H2Bz4Me or 1 : 1 [Zn(HL)Cl$_2$] with H2Bz4Ph; all contain a neutral thiosemicarbazone and two chloride ions coordinated to the metal, as indicated by the molar conductivity measurements.

The infrared spectral bands most useful for determining the mode of coordination are given in table 3. The ν(C=N) bands of the thiosemicarbazones at 1585–1615 cm^{-1} shift in the spectra of the complexes to 1560–1595 cm^{-1}, indicating coordination of the azomethine nitrogen [11–13]. The uncomplexed thiosemicarbazones show the thioamide IV band in the 800–805 cm^{-1} range. This band shifts to 780–797 cm^{-1} in the zinc(II) and iron(II) complexes as well as in complex **6**, suggesting coordination of a thione sulphur [20]. In the spectra of complexes **4** and **5** an absorption is observable at 749–758 cm^{-1}, indicating the presence of a thiolate sulphur [12, 13]. The in-plane-deformation mode of pyridine at 590–595 cm^{-1} in the spectra of the ligands shifts 45–63 cm^{-1} to higher frequencies in complexes **1**–**5**, indicating coordination of the heteroaromatic nitrogen [12] but only 0–10 cm^{-1} in complexes **6**–**9**, suggesting that in the latter the heteroaromatic nitrogen is not involved in complexation. Therefore, the infrared data indicate coordination of the thiosemicarbazone through the N$_{py}$–N(2)–S tridentate chelating system in the case of complexes **1**–**5** and through the bidentate N(2)–S system in complexes **6**–**9**. In addition, absorptions at 345–470 cm^{-1}, 335–375 cm^{-1}, 254–302 cm^{-1} and 277–293 cm^{-1} in the spectra of the complexes were assigned to the M–N, M–S, M–Cl and M–Npy vibrations, respectively [12–14]. For zinc(II) complexes two absorptions attributable to the M–Cl vibration are observed, suggesting that the chlorides are *cis* [21].

The Mössbauer spectra of the iron complexes (figure 3) are characteristic of low spin iron(II). The room temperature isomer shift relative to metallic iron (δ) and quadrupole splitting (Δ) are: $\delta = 0.24 \pm 0.01\,\mathrm{mm\,s^{-1}}$, $\Delta = 0.39 \pm 0.02\,\mathrm{mm\,s^{-1}}$ (**1**); $\delta = 0.23 \pm 0.01\,\mathrm{mm\,s^{-1}}$, $\Delta = 0.40 \pm 0.02\,\mathrm{mm\,s^{-1}}$ (**2**) and $\delta = 0.21 \pm 0.01\,\mathrm{mm\,s^{-1}}$, $\Delta = 0.58 \pm 0.02\,\mathrm{mm\,s^{-1}}$ (**3**). These parameters are compatible with the parameters obtained

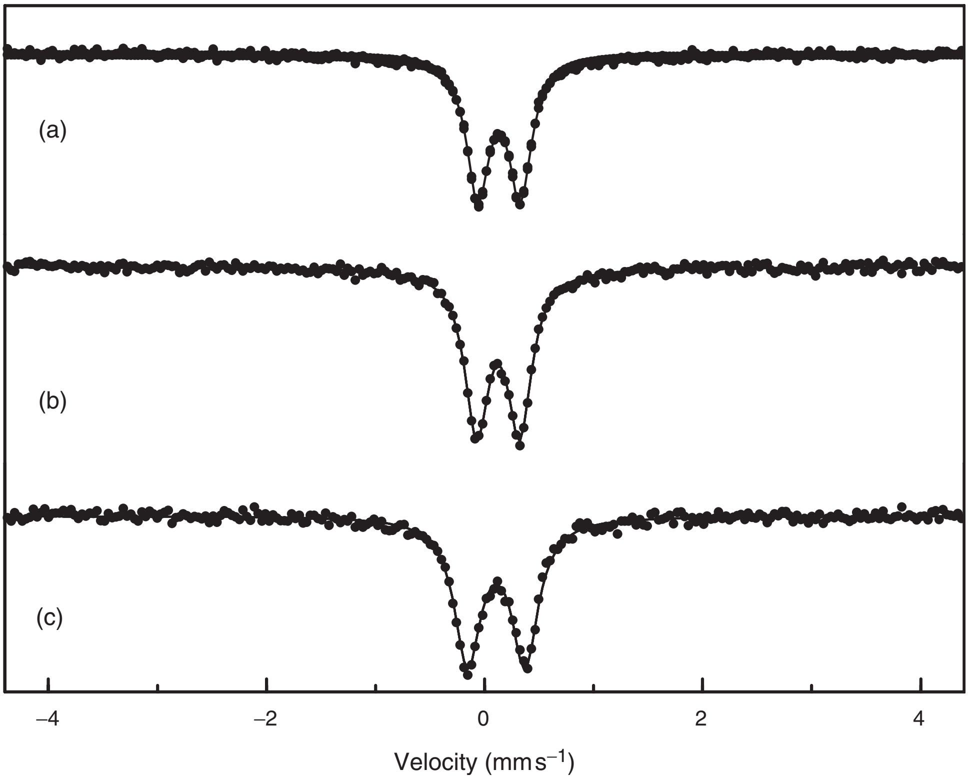

Figure 3. Mössbauer spectra of (a) $[Fe(H2Bz4DH)_2]Cl_2$ (**1**); (b) $[Fe(H2Bz4Me)_2]Cl_2$ (**2**); (c) $[Fe(H2Bz4Ph)_2]$ Cl_2 (**3**).

previously for the iron(II) complexes of 2-formylpyridine ($\delta = 0.24 \pm 0.02\,\mathrm{mm\,s^{-1}}$, $\Delta = 0.48 \pm 0.02\,\mathrm{mm\,s^{-1}}$) and 2-acetylpyridine ($\delta = 0.264 \pm 0.001\,\mathrm{mm\,s^{-1}}$, $\Delta = 0.537 \pm 0.002\,\mathrm{mm\,s^{-1}}$) thiosemicarbazones [8, 9]. The increasing values of Δ in going from complexes **1** and **2** to complex **3** are probably due to increased distortions in the symmetry of charge density resulting from the greater bulkiness of the N(4)-group.

Table 4 lists the ^{1}H- and ^{13}C-NMR shift values and assignments for the thiosemicarbazones and their zinc(II) complexes in DMSO-d$_6$. The ^{1}H resonances were assigned based on chemical shifts, multiplicities and coupling constants. The carbon type (C, CH) was determined by using DEPT135 experiments.

In the spectra of the thiosemicarbazones the signals are doubled as a consequence of the existence of the *Z* and *E* configurational isomers (figure 1) in solution. Other authors report the presence of the *Z* isomer of 2-benzoylpyridine N(4)-alkyl thiosemicarbazones in $CDCl_3$ solution but do not report the coexistence of both forms [11, 12]. In previous work the existence of these two isomers for H2Bz4Ph are reported [14], for which N(3)–H is hydrogen bonding to the pyridine nitrogen in the *Z* configuration and its signal appears at $\delta = 13.09$. In the *E* form this signal is observed at $\delta = 10.57$, indicating hydrogen bonding to the solvent [22]. Similarly, for H2Bz4DH and H2Bz4Me all signals are doubled. The resonances of N(3)–H are found at $\delta = 12.51$ and $\delta = 12.85$, respectively, characteristic of the *Z* configuration, and at $\delta = 8.61$ and

Table 4. ^{1}H- and ^{13}C-NMR assignments and shift values of 2-benzoylpyridine thiosemicarbazones and their Zn(II) complexes (DMSO-d$_6$).

	H2Bz4DH		H2Bz4Me		H2Bz4Ph		[Zn(H2Bz4DH)$_2$Cl$_2$] (**7**)	[Zn(H2Bz4Me)$_2$Cl$_2$] (**8**)	[Zn(H2Bz4Ph)Cl$_2$] (**9**)
	Z	*E*	*Z*	*E*	*Z*	*E*	*Z*	*Z*	*Z*
N(3)H	12.51 (s)	8.61 (s)	12.85 (s)	8.67 (s)	13.09 (s)	10.57 (s)	12.53 (s)	12.79 (s)	13.05 (s)
N(4)H	8.63 (s) 8.20 (s)	8.78 (s) 8.47 (s)	8.72–8.63 (m)	8.99–8.9 (m)	10.31(s)	8.97 (s)	8.60 (s, b)	8.72 (d, b)	10.31 (s)
H6	8.86 (d)	8.45 (d)	9.86–8.83 (m)	8.73–8.69 (m)	8.87 (d)	8.45 (d)	8.85 (d)	8.84 (d)	8.87 (d)
C=S	178.56	177.99	178.02	177.57	176.51	176.34	178.57	178.06	176.67
C=N	151.08	154.36	151.48	154.40	151.38	154.30	151.38	151.47	151.20

Note: s, singlet; d, doublet; m, multiplet; b, broad.

Table 5. Solution (DMF) electronic spectra (cm^{-1}) of the Fe(II) and Ni(II) complexes of 2-benzoylpyridine thiosemicarbazones.

Compound	Intraligand and charge transfer transitions	d–d Transitions
H2Bz4DH	29670	
H2Bz4Me	29150	
H2Bz4Ph	29240	
$[Fe(H2Bz4DH)_2]Cl_2$ (**1**)	31060–29595–23201–19230–16180	13700–12760
$[Fe(H2Bz4Me)_2]Cl_2$ (**2**)	30960–26180–23810–18080–16130	13420–10990
$[Fe(H2Bz4Ph)_2]Cl_2$ (**3**)	25250–23260–17860–15670	13170–11150
[Ni(2Bz4DH)Cl] (**4**)	31150–25250–23480	12660–11560
[Ni(2Bz4Me)Cl] (**5**)	25970–23560	12660–11630
$[Ni(H2Bz4Ph)_2]Cl_2$ (**6**)	30770–29030–25260–22880	12500–11430–11240

$\delta = 8.67$ respectively, for the *E* configuration. In the latter, hydrogen bonding to the solvent is possible (the signal of N(3)–H in $CDCl_3$ is found at ca $\delta = 7.5$ for both compounds) but it would not be as strong as for H2Bz4Ph.

In the spectra of H2Bz4Me and H2Bz4Ph the two configurations are present immediately after dissolution but the *E*-form only appears after 1 h in the spectrum of H2Bz4DH, indicating that *E*-isomer formation is faster for the former two compounds.

The nickel(II) complexes are paramagnetic, as suggested by their very broad NMR signals (not shown) and hence approximately tetrahedral or distorted square planar. However, the presence of a signal at $\delta = 12.81$ for complex **6**, attributed to N(3)–H as well as its absence in the spectra of complexes **4** and **5** confirms the presence of a neutral ligand in the first case and of an anionic thiosemicarbazone in the latter. Moreover, the high frequency N(3)–H signal indicates the presence of the thiosemicarbazone in the *Z* configuration in complex **6**, which leads to bidentate coordination through N(2)–S, in agreement with the infrared data.

In the ^{1}H- and ^{13}C-spectra the chemical shifts show small differences upon coordination to zinc(II), probably due to its d^{10} configuration, which does not favour the transfer of electron density from the ligand to the metal centre. However, in the spectra of the complexes only one signal is observed for all hydrogens and carbons, indicating the existence of only one configuration. N(3)–H is found at $\delta = 12.53$, $\delta = 12.79$ and $\delta = 13.05$ for complexes **7**, **8** and **9** respectively, consistent with the presence of the thiosemicarbazone in the *Z* form, in agreement with bidentate coordination, as suggested by the infrared data. All other signals are compatible with a *Z* configuration.

Table 5 lists the solution (DMF) electronic spectral data for the thiosemicarbazones and their iron(II) and nickel(II) complexes. The data for the zinc(II) complexes are omitted due to the similarity of their spectra to those of the ligands. The $\pi \rightarrow \pi^*$ transitions of the thiosemicarbazone moieties at 36,370–37,000 cm^{-1} are not significantly altered upon complexation and were omitted from table 5. The $n \rightarrow \pi^*$ transitions of the azomethine and thioamide functions [13] merge in the spectra of the free thiosemicarbazones at 29,150–29,670 cm^{-1} and shift to 30,770–31,150 cm^{-1} and 25,250–25,970 cm^{-1} in the nickel(II) complexes. Additional bands between 22,880 and 23,560 cm^{-1} in the spectra of the nickel(II) complexes are associated with $S(\sigma, \pi) \rightarrow$ Ni(II) charge transfer transitions [13]. Absorptions in the 11,240–12,660 cm^{-1} range were attributed to d–d transitions [23, 24]. For the iron(II) complexes the two $n \rightarrow \pi^*$ transitions are observed in the 30,960–31,060 cm^{-1} and

Table 6. Cyclic voltammetry data for the iron complexes with 2-benzoylpyridine thiosemicarbazones.

Compound	E° (V)	i_{pc}/i_{pa}
$[Fe(H2Bz4DH)_2]Cl_2$ (**1**)	−0.28	1.31
$[Fe(H2Bz4Me)_2]Cl_2$ (**2**)	−0.23	1.13
$[Fe(H2Bz4Ph)_2]Cl_2$ (**3**)	−0.22	1.12

26,180–29,590 cm^{-1} ranges. For complex **3** these two absorptions overlap at 25,250 cm^{-1}. The absorptions in the 23,201–23,810 cm^{-1} range may be attributed to $S(\sigma, \pi) \rightarrow$ iron(II) charge transfer transitions, and those in the 15,670–16,180 cm^{-1} range to iron(II) metal-to-ligand charge transfer transitions [21]. A shoulder at 17,860–19,230 cm^{-1} is attributed to a vibronic structure corresponding to a transition to an excited vibrational level [7]. The d–d transitions are observed in the 10,990–13,700 cm^{-1} range [21].

In aqueous solution (1.0×10^{-4} mol L^{-1}) the complexes exhibit a band at ca 16,700 cm^{-1}, attributed to an iron(II) metal-to-ligand charge transfer [21]. Over time the intensity of this maximum decreases and a new absorption appears at ca 22,200 cm^{-1}, attributed to an iron(III) metal-to-ligand charge transfer. Upon addition of dithiothreitol (DTT, $CH_2SH(CHOH)_2CH_2SH$), this absorption disappears and the spectra of the iron(II) complexes are recovered (data not shown). DTT is a cellular thiol-like reducing agent, which acts as a model of the reducing substrate of RDR, in the place of thioredoxine.

Electrochemical oxidation and reduction of the iron(II) complexes of 2-benzoylpyridine thiosemicarbazones were studied in DMF solution using cyclic voltammetry. Table 6 lists cyclic voltammetry data for $[Fe(H2Bz4DH)_2]Cl_2$ (**1**), $[Fe(H2Bz4Me)_2]Cl_2$ (**2**) and $[Fe(H2Bz4Ph)_2]Cl_2$ (**3**). Figure 4 shows the cyclic voltammograms for the iron(II) complexes at 100 mV s^{-1}.

The cyclic voltammograms of the ligands exhibit waves near the more negative margin (cathodic peak potential, E_{pc}, reduction in the −0.98 to 0.87 V range, data not shown), which were attributed to reduction of the conjugated portion of the thiosemicarbazone, in agreement with data obtained in the literature for other thiosemicarbazones in the same solvent [25]. Early work reported an electrochemical study of H2Bz4DH but the solvent used was ethanol [26].

The three iron complexes exhibit high electrochemical stability with $[Fe(H2Bz4Ph)_2]Cl_2$ (**3**) the most stable. For the three complexes, studies at different scan rates (between 10 and 200 mV s^{-1}) indicated a linear dependence of the anodic and cathodic peak current with the square root of the scan rate, which confirms the quasi-reversibility of the charge transfers that are controlled by diffusion.

The cyclic voltammograms of the iron complexes are characteristic of one-electron redox systems. The observed peaks are assigned to the Fe(III)/Fe(II) couple. The apparent formal potential, E°, was calculated using the approximation $E^\circ = 1/2(E_{pa} + E_{pc})$, in which E_{pa} and E_{pc} stand for the anodic and cathodic peak potentials, respectively. Table 6 lists the apparent formal potential and the ratio between the anodic peak current to the cathodic peak current, i_{pa}/i_{pc}.

For all three compounds the separation between the main reduction peak and its counterpart is characteristic of a quasi-reversible one-electron system. For $[Fe(H2Bz4Me)_2]Cl_2$ (**2**) and $[Fe(H2Bz4Ph)_2]Cl_2$ (**3**) close values of i_{pc}/i_{pa} were observed,

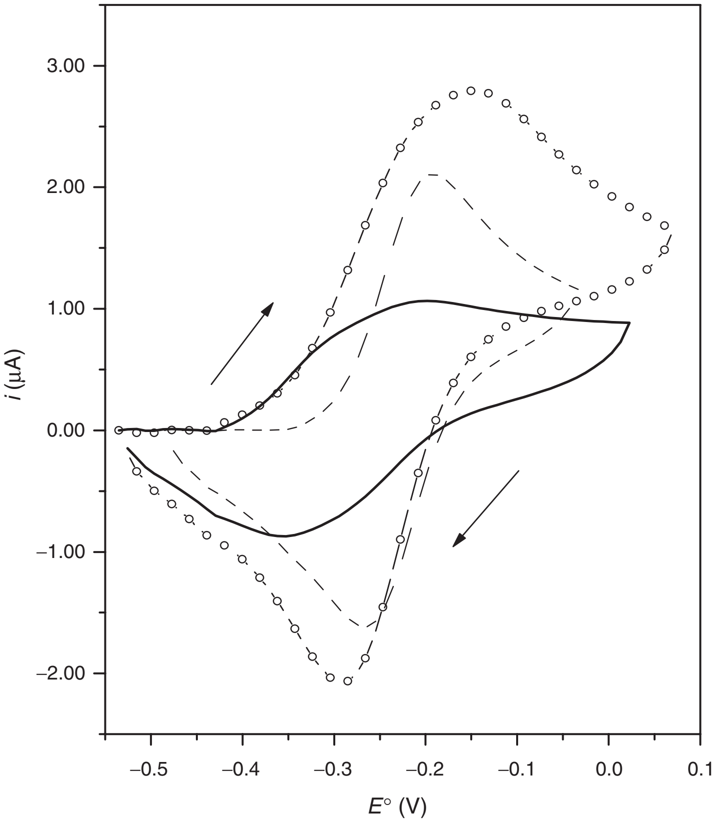

Figure 4. Cyclic voltammograms (100 mV s^{-1}) for [Fe(H2Bz4DH)$_2$]Cl$_2$ (**1**) (—), [Fe(H2Bz4Me)$_2$]Cl$_2$ (**2**) (– ○ –), [Fe(H2Bz4Ph)$_2$]Cl$_2$ (**3**) (– – –), in DMF solution containing 0.1 M TBATFB. The potentials are *vs.* NHE.

of the order of 1.12–1.13, while for [Fe(H2Bz4DH)$_2$]Cl$_2$ (**1**) it was found that $i_{pc}/i_{pa} = 1.32$, indicating a more irreversible system [27].

The values of the apparent formal potential are similar for the three complexes. These potentials are accessible by cellular thiols, for which the oxidation potential is generally found around 0.25–0.27 V [28]. The potential for [Fe(H2Bz4Ph)$_2$]Cl$_2$ (**3**) is the least negative, suggesting an easier reductive attack of this complex by cellular thiols.

It has already been shown that RDR contains a stable electron deficient tyrosyl radical that disappears by inactivation of the enzyme [29]. In previous work it has been suggested that the mechanism of antitumoral action of 2-formylpyridine thiosemicarbazone or its iron complexes could involve oxidation of the iron(II) to the iron(III) complex with release of one electron to the free radical of RDR and inactivation of the enzyme, followed by reduction of the iron(III) complex by a cellular thiol [7, 8] such as glutathione or the RDR substrate thioredoxine.

The measured potentials of these iron complexes are similar to those found in the literature for the iron(II) complex of the antitumoral agent 2-formylpyridine thiosemicarbazone ($E^\circ = -0.24$ V) [30] indicating the antitumoral properties of the 2-benzoylpyridine thiosemicarbazones or their iron complexes should be investigated.

The growth inhibition zone of *Candida albicans* yeast in the presence of the thiosemicarbazones and their metal complexes has been determined. The N(4)-substituted thiosemicarbazones seem to be slightly more effective than the unsubstituted compound, probably due to increased lipophilicity. For example, at 6400 ppm, the growth inhibition zones were 9.5, 10.5 and 11.0 mm for H2Bz4DH, H2Bz4Me and H2Bz4Ph, respectively (6.0 mm = no inhibition). In addition, at 10,000 ppm they were 15.5 and 18.0 mm for H2Bz4DH and H2Bz4Me, respectively (H2Bz4Ph is insoluble). Upon coordination to iron(II), nickel(II) and zinc(II) the activity is lost or decreases significantly (growth inhibition zone = 6.0–7.0 mm). It has been proposed that ligands may act by inhibiting enzymes necessary to the fungus metabolism whose activity depends on metals [31]. In the present case, if the thiosemicarbazones are already coordinated, they are unavailable for further complexation.

Supplementary data

Crystallographic data for H2Bz4Me have been deposited at Cambridge Crystallographic Data Centre (CCDC) as supplementary publication number CCDC 248528. Copies of available material can be obtained on application to CCDC, 12 Union Road, Cambridge CB2 1EZ, UK (fax: 44-1223-336033 or email: deposit@ccdc. cam.ac.uk).

Acknowledgements

Financial support from the Brazilian funding agencies CNPq, Capes and Fapemig is acknowledged.

References

[1] H. Beraldo, D. Gambino. *Mini Rev. Med. Chem.*, **4**, 31 (2004).
[2] J.P. Scovill, D.L. Klaymann, C.F. Franchino. *J. Med. Chem.*, **25**, 1261 (1982).
[3] R.A. Finch, M. Liu, S.P. Grill, W.C. Rose, R. Loomis, K.M. Vasquez, Y. Cheng, A.C. Sartorelli. *Biochem. Pharmacol.*, **59**, 983 (2000).
[4] D.X. West, S.B. Padhye, P.B. Sonawane. *Struct. Bond.*, **76**, 1 (1991).
[5] H. Beraldo, L. Tosi. *Inorg. Chim. Acta*, **75**, 249 (1983).
[6] H. Beraldo, L. Tosi. *Inorg. Chim. Acta*, **125**, 173 (1986).
[7] R.H.U. Borges, E. Paniago, H. Beraldo. *J. Inorg. Biochem.*, **65**, 268 (1997).
[8] A. Abras, H. Beraldo, E. Fantini, R.H.U. Borges, M.A. da Rocha, L. Tosi. *Inorg. Chim. Acta*, **172**, 113 (1990).
[9] R.H.U. Borges, A. Abras, H. Beraldo. *J. Braz. Chem. Soc.*, **8**, 33 (1997).
[10] De. Kuntala, A.K. Guha. *Indian J. Chem. Sect. A*, **29**, 605 (1990).
[11] D.X. West, J.S. Ives, J. Krejci, M.M. Salberg, T.L. Zumbahlen, G.A. Bain, A.E. Liberta. *Polyhedron*, **14**, 2189 (1995).
[12] D.X. West, A.M. Stark, G.A. Bain, A.E. Liberta. *Trans. Met. Chem.*, **21**, 289 (1996).
[13] D.X. West, I.S. Billeh, J.P. Jasinski, J.M. Jasinski, R.J. Butcher. *Trans. Met. Chem.*, **23**, 209 (1998).
[14] A. Perez-Rebolledo, G.M. de Lima, L.N. Gambi, N.L. Speziali, D.F. Maia, C.B. Pinheiro, J.D. Ardisson, M.E. Cortés, H. Beraldo. *Appl. Organometal. Chem.*, **17**, 945 (2003).
[15] Enraf-Nonius, Nonius, B.V. *Collect*, Delft, The Netherlands (1997–2000).
[16] Z. Otwinowski, W. Minor. In *Methods in Enzymology*, C.W. Carter, R.M. Sweet (Eds), Vol. 276, pp. 307–326, Academic Press, New York (1997).
[17] G.M. Sheldrick. *SHELXS-97, Program for the Solution of Crystal Structures*, University of Göttingen, Germany (1997).

[18] G.M. Sheldrick. *SHELXL-97, Program for Crystal Structures Analysis*, University of Göttingen, Germany (1997).

[19] H. Beraldo, A. Mena Barreto, R.P. Vieira, A.P. Rebolledo, N.L. Speziali, C.B. Pinheiro, G. Chapuis. *J. Mol. Struct.*, **645**, 213 (2003).

[20] R.L. Lima, L.R.S. Teixeira, T.M. Gomes Carneiro, H. Beraldo. *J. Braz. Chem. Soc.*, **10**, 184 (1999).

[21] K. Nakamoto. *Infrared and Raman Spectra of Inorganic and Coordination Compounds*, John Wiley & Sons, New York (1986).

[22] I.M.C. Mendes, L.R. Teixeira, R.L. Lima, T.M. Carneiro, H. Beraldo. *Trans. Met. Chem.*, **24**, 665 (1999).

[23] H. Beraldo, L.P. Boyd, D.X. West. *Trans. Met. Chem.*, **23**, 67 (1998).

[24] A.B.P. Lever. *Inorganic Electronic Spectroscopy*, Elsevier, Amsterdam (1984).

[25] D. Kovala-Demertzi, A. Domopoulou, M.A. Demertzis, A. Papageorgiou, D.X. West. *Polyhedron*, **16**, 3625 (1997).

[26] M.A. Gómez Nieto, M.D. Luque de Castro, M. Valcarcel. *Electrochim. Acta*, **27**, 435 (1982).

[27] A.L. Bard, L.R. Faulkner. *Electrochemical Methods: Fundamentals and Applications*, John Wiley & Sons, New York (2001).

[28] D.H. Petering. *Bioinorganic Chem.*, **1**, 273 (1972).

[29] L. Thelander, A. Gräslund. *J. Biol. Chem.*, **256**, 4063 (1983).

[30] J.M. Knight, H. Whelan, D.H. Petering. *J. Inorg. Biochem.*, **11**, 327 (1979).

[31] N. Fahmi, R.V. Singh. *J. Indian Chem. Soc.*, **73**, 257 (1996).